Raport Badawczy
Research Report

RB/03/2001

Forecasting of sulfur deposition on a regional scale

P. Holnicki, A. Żochowski,
K. Abert, K. Juda-Rezler

Instytut Badań Systemowych
Polska Akademia Nauk

Systems Research Institute
Polish Academy of Sciences

POLSKA AKADEMIA NAUK

Instytut Badań Systemowych

ul. Newelska 6

01-447 Warszawa

tel.: (+48) (22) 8373578

fax: (+48) (22) 8372772

Pracę zgłosił: dr inż. Piotr Holnicki

Warszawa 2001

Forecasting of sulfur deposition on a regional scale

Piotr Holnicki [1], *Antoni Żochowski* [1], *Krzysztof Abert* [2] *and Katarzyna Juda-Rezler* [2]

[1]) *Systems Research Institute*
Polish Academy of Sciences
Warsaw

[2]) *Warsaw University of Technology*
Institute of Environmental Engineering
Systems, Warsaw

Keywords: environment protection, sulfur deposition, mathematical modeling

Abstract: The paper presents an algorithm for the prediction of regional scale sulfur deposition. The method is based on a dynamic, single-layer model of air pollution dispersion. The set of two transport equations, for the primary (SO_2) and secondary ($SO_4^=$) sulfur species is solved. Finally, the model generates spatial characteristics of the cumulated sulfur deposition due to transport and deposition processes, taking into account aerodynamical parameters of the terrain and chemical transformations.

The model is aimed at evaluation of sulfur deposition originating from the major emission sources, representing the sector of energy generation. The emission intensity of each source and the time sequence of meteorological parameters within the period of simulation constitute the main input data. The model computes the contribution of each source to sulfur deposition over the prescribed time interval. The resulting total deposition map is a sum of individual contributions. The land-cover characteristics is an important factor in this calculation.

Test computations were performed for the set of major power plants in Poland using two estimation methods of dry deposition velocity for SO_2: (i) the standard literature value and (ii) the variable value, calculated due to the modified version of RIVM's dry deposition model (Erisman et al., 1994). The presented results refer to seasonal winter and summer depositions as well as the total annual value.

1 The transport model formulation

The process of computing deposition forecast utilizes the discrete in time procedure, which simulates dynamics of air pollution dispersion. The basic input data contain emission intensity of each source (constant over a season) and time-variable meteorological parameters. The latter are entered as a sequence of the measurement data for each time step. Calculations performed in each time interval consist of two basic stages:

- evaluation of SO_2 and $SO_4^=$ concentrations,
- evaluation of total sulfur deposition resulting from the current concentration, meteorological data and the land-cover characteristics.

Concentration forecasts of the main pollution components are generated by a single-layer dispersion model, based on the transport equations (Lyons and Scott, 1990). The model is of Lagrangian-type and the computational technique is based on the method of characteristics. The mass balance of pollutants is calculated in each grid element for air parcels following the wind trajectories. The approach is source-oriented, thus the trajectory, which starts at the specific emission source, is observed until the mass of the parcel drops below 1% of its initial value or the parcel leaves the computational area. The procedure is applied in turn to all the individual sources, and the resulting concentrations are summed up to give the total concentration map in the current time step. Furthermore, the sulfur deposition in the consecutive time steps is calculated as a function of the current concentration, meteorological conditions and physical deposition parameters.

1.1 The governing equations of the transport model

For computational purposes, the problem is formulated as a discrete in time with homogeneous spatial resolution of the domain. The uniform space discretization step will be denoted by $h = \Delta x = \Delta y$. Points along the trajectory are determined at discrete time moments, based on the interval τ, which in our computation was taken 15 min. The main output of the first stage of simulation constitute the primary (SO_2) and secondary ($SO_4^=$) concentrations, averaged over the discretization element and the mixing layer height. They finally yield the deposition contribution in the consecutive time steps.

The initial concentrations depend on the emission intensity of a specific source and are calculated according to the formulae

$$q_1 = \frac{(1-\beta)E\tau}{HM \cdot h^2}\,, \tag{1}$$

$$q_2 = \frac{\beta E\tau}{HM \cdot h^2}\,, \tag{2}$$

where q_1, q_2 denote concentrations of SO_2 and $SO_4^=$ in [μg m^{-3}], E is total sulfur emission of this source [g s^{-1}], β – fraction emitted directly as $SO_4^=$, HM – the mixing layer height in [m].

The continuity equations for both components reflect spatial and temporal transformation of this initial value. They include advective transport, chemical transformations $SO_2 \Longrightarrow SO_4^=$, dry deposition and scavenging by precipitation.

$$\frac{\partial q_1}{\partial t} + \vec{w}\,\nabla q_1 + (k_{d_1} + k_{w_1})\,q_1 + k_t\,q_1 = 0\,, \tag{3}$$

$$\frac{\partial q_2}{\partial t} + \vec{w}\,\nabla q_2 + (k_{d_2} + k_{w_2})\,q_2 = k_t\,q_1\,, \tag{4}$$

where
k_{d_i} – dry deposition coefficient [s^{-1}], k_{w_i} – coefficient of wet deposition due to scavenging

by precipitation [s^{-1}], k_t – coefficient of chemical transformation $SO_2 \Longrightarrow SO_4^=$ [s^{-1}], $\vec{w} = [u, v]$ – wind velocity vector [m s^{-1}]. The emission term does not appear on the right-hand side of (3) and (4), since the model simulates dispersion and environmental impact (spatial and temporal) of the initial concentrations (1) and (2), related to a source.

The transition from $q_i(t)$ to $q_i(t+\tau)$ i=1,2, is split into two steps, representing:

i) advective transport using trajectory following technique,

ii) changes of concentrations of pollutants in the air due to chemical transformations and deposition.

The second step may be performed analytically.

Assuming the coefficients in (3), (4) constant over the interval [t,t+τ], one can express the respective solutions in the following form (compare Sandnes, 1993)

$$q_1(t+\tau) = q_1(t)\exp(-(k_{d_1} + k_{w_1} + k_t))\tau \qquad (5)$$

$$q_2(t+\tau) = \frac{k_t\, q_1(t)}{k_{d_2} + k_{w_2}}\,[1 - \exp(-(k_{d_2} + k_{w_2})\tau] + q_2(t)\exp(-(k_{d_2} + k_{w_2}))\tau \qquad (6)$$

The coefficients, which represent the decline due to dry deposition in (3) – (6) are defined as follows:

$$k_{d_i} = \frac{v_{d_i}}{HM}, \qquad \text{for} \quad i = 1, 2, \qquad (7)$$

where the dry deposition velocity for SO_2 – v_{d_1},(in [m s^{-1}]), is preprocessed by a specialized RIVM's algorithm (Erisman, 1992; Erisman *et al.*, 1994; van Pul, 1994), modified by the Institute of Environmental Engineering Systems (Warsaw Institute of Technology). The input data of this algorithm, discussed in Section 2 in more details, consists of the meteorological forecast and physical parameters of the domain, e.g. the land-cover characteristics. An alternative approach is applying the constant value v_{d_1}=0.008 [m s^{-1}]. In Section 3 case study results for these two approaches are compared. Moreover, basing on the solution presented by Sandnes (1993), dry deposition velocity for $SO_4^=$ is assumed $v_{d_2} = 0.2 v_{d_1}$.

Wet deposition depends in our model on precipitation intensity and is expressed, in general, as

$$k_{w_i} = \frac{\Lambda_i P}{HM} = \frac{w_{d_i}}{HM}, \qquad \text{for} \quad i = 1, 2. \qquad (8)$$

Here P denotes the precipitation height in [mm], accumulated over the time interval. Following Sandnes (1993), the scavenging factor for SO_2 can reflect seasonal fluctuations of the air temperature and is parameterized as follows

$$\Lambda_1 = 3 \cdot 10^5 + 1 \cdot 10^5 \sin[2\pi(T - T_0)/T_a]\,. \qquad (9)$$

T represents here the current day of the year, T_0 = 80 days – the reference date, and T_a = 365 days. For simplicity, the scavenging factor for $SO_4^=$ is assumed constant (Sandnes, 1993),

$$\Lambda_2 = 1 \cdot 10^6\,. \qquad (10)$$

In an analogous way, the chemical transformation coefficient in (3) – (6) can be defined according to the formula

$$k_t = a_t + b_t \sin[2\pi(T - T_0)/T_a]. \qquad (11)$$

where the parameters a_t, b_t are constant,

$$a_t = 3 \cdot 10^{-6} \quad [s^{-1}], \qquad b_t = 2 \cdot 10^{-6} \quad [s^{-1}],$$

while T, T_0 and T_a are defined as in (9).

Concentrations q_1 and q_2 of SO_2 and $SO_4^=$ constitute the output from the first stage the model. The averaged over time-step concentrations are then used to calculate depositions in the consecutive steps of the algorithm. For the primary and secondary type pollution they are as follows:

$$D_i = (v_{d_i} + w_{d_i}) \cdot q_i \cdot \tau \qquad \text{for} \qquad i = 1, 2. \qquad (12)$$

Finally, the contributions of the consecutive time steps are summed up to give the total sulfur deposition over the interval of simulation.

1.2 The wind-field trajectories preprocessing

The wind field in the computational region within the time interval of the forecast is the basic meteorological input of the pollution transport model. Since air transport model represents a single-layer approach, the wind should also be averaged over the mixing layer approximation of the three-dimensional field. It should moreover reflect the dynamics of temporal changes within the forecasting interval. The aim of this module of the algorithm is to generate wind-field trajectories, which are next used in simulation of pollution transport.

The trajectory generation procedure uses the following input data: (i) a complete set of wind field measurements in selected field stations, (ii) the coordinates of emission sources location. The approach applied is based on the spatial and temporal interpolation of the sequence of meteorological data obtained from selected measurement stations. Each station records the set of data twice a day; the time interval is ΔT=12 h. The set of measurement data contains the following wind characteristics:

- components of the anemometric wind u_A, v_A,
- components of the geostrophic wind (850 hPa) u_G, v_G.

The above data have to be spatially and temporarily interpolated over the computational domain. The resulting wind field, averaged over the mixing layer, should also reflect some additional constraints. One of them, imposed due to the general model of atmospheric circulation, is the continuity condition of the following form:

$$\frac{\partial u}{\partial x} + \frac{\partial v}{\partial y} = 0. \qquad (13)$$

The field is preprocessed by the spatial interpolation of the measured input data, and time interpolation of the consecutive episodes. The approach applied in the interpolation algorithm is based on the assumption, that the movement of the atmosphere has the rotational character – it rotates around certain centers located in regions of high or low pressure. The wind components in such a field satisfy the following relation:

$$[u(x,y), v(x,y)] = k \cdot [-(y - y_0), (x - x_0)]\,, \tag{14}$$

where point (x_0, y_0) denotes the center of the vortex.

Some simplifications are made in the trajectory model. Due to the single-layer structure of the dispersion model, the vertical movement of air masses has been neglected, and the horizontal transport of the pollutant cloud at the average height of about 150 meters is considered. In the simplified version, the influence of orography on the wind streamlines is neglected (the full model computes the respective wind vector corrections). The trajectory is evaluated for an individual package of pollutant, emitted by a source.

Denoting by (x_p, y_p) the coordinates of the current position of a pollutant package, the equations of its trajectory have the form:

$$\begin{aligned} \frac{dx_p}{dt} &= u(x_p, y_p, t)\,, \qquad x_p(0) = x_0\,, \\ \frac{dy_p}{dt} &= v(x_p, y_p, t)\,, \qquad y_p(0) = y_0\,, \end{aligned} \tag{15}$$

where (x_0, y_0) is the initial position of the package.

The solution algorithm is based on the simple difference approximation. For the time discretization step τ, one obtains

$$\begin{aligned} x_p((k+1)\tau) &= x_p(k\tau) + \tau u(x_p(k\tau), y_p(k\tau), k\tau)\,, \\ y_p((k+1)\tau) &= y_p(k\tau) + \tau v(x_p(k\tau), y_p(k\tau), k\tau)\,. \end{aligned} \tag{16}$$

Since the values of the wind velocity components u and v are measured only every 12 hours, the time interval ΔT has to be additionally discretized due to computational purposes. Therefore, the two time scales are applied:

- the division of the forecast horizon (e.g. one year) into N 12-hour intervals ΔT.
- the division of each interval ΔT into m time-steps of the length τ, i.e.

$$\Delta T = m\tau\,.$$

Thus, the total time period of the forecast is $T_N = m \cdot N \cdot \tau$. At the end of each time interval $(i\Delta T, (i+1)\Delta T)$ we know the wind measurements in meteorological stations. For the moment $t_{i,j} = i\Delta T + j\tau$, $(j < m)$, we must perform the interpolation of the wind vector $\vec{w} = [u, v]$ between two consecutive values: $\vec{w}(i\Delta T)$ and $\vec{w}((i+1)\Delta T)$.

The simplest linear interpolation is inadequate in this case. For example, the rotation of the wind field by the angle close to π could cause the temporary lack of wind. Moreover, the direction of the wind vector rotation has to be taken into account in the interpolation procedure. Thus, the direction and the speed of wind in each step are interpolated separately. The procedure includes a special algorithm identifying the direction in which the wind vector rotates.

Given the values of the wind vector at every time moment at the measuring stations, the wind components at any selected point of the computational domain are calculated by means of the interpolation procedure described above in the formulae (13)-(16). As a result we obtain the trajectory of the pollutant package up to the point when it leaves the computational area, or vanishes (the total mass of the package drops below 1% of its initial value) due to chemical transformations or deposition of pollutants.

Using the above algorithm, we know the current position of pollutant package originating from any single emission source at any time point of the integration interval. This information is next utilized for calculation of the pollution concentration involved by the observed package in the consecutive elements of area discretization.

An important drawback of a single-layer approximation of a three-dimensional transport is related to unrealistically high concentration values in the neighborhood of high stacks. This effect is reduced by an evaluation of the initial plume rise and the effective stack height, applied for all the sources under consideration. The effective stack height is calculated according to Holland formula (Lyons and Scott, 1990), and the initial development of the pollutant package is parameterized by an artificial shift of the emission source coordinates. Justification of this approach is related to the main task of the model discussed here – the calculation of sulfur deposition, since from this point of view we are interested in finding the place, where the pollutant cloud first touches the earth surface.

The other meteorological fields (precipitation, relative humidity, temperature) are approximated by the stepwise functions; the respective values are constat in subdomains represented by the closest meteorological station (the Voronoy's scheme).

2 Model of dry deposition

In order to improve the predictions of the transport model, the detailed dry deposition submodel has been used. The SO_2 concentrations strongly depend on dry deposition process, so its parameterization is essential for the model results. The dry deposition submodel for sulfur species, based on the original multi-species RIVM's (National Institute of Public Health and Environmental Protection, Bilthoven, the Netherlands) dry deposition model (Erisman *et al.*, 1994; van Pul, 1994), has been developed and tested. The original RIVM's model, named DEPAC, considers seven sulfur and nitrogen species. For the purposes of current work only the part dealing with sulfur dioxide have been extracted. Model sensitivity to its input parameters has been extensively tested. Analysis of test results allowed for neglecting of some input parameters. Thus, the modified version of the SO_2 dry deposition submodel prepared for implementation with sulfur air pollution

trajectory model used in current work has been developed. The dry deposition velocity v_d represents the ability of the given land cover to absorb given pollutant under specific meteorological conditions. Adequate parameterization of the v_d is very important as both concentration and deposition values depend on that value. For the majority of pollutant v_d strongly varies in time and space. Dry deposition of gases from the atmosphere to the ground comprises three stages: first, the material must be transported through the atmosphere to the receptor surface (turbulent layer); second, there occur transport through the quasi-laminar layer at the surface; last, the gas must be captured by the surface (Voldner *et al.*, 1986; Erisman, 1992). Thus, to account for these three stages of deposition process, the parameterization of v_d in the dry deposition model is based on the resistance analogy.

$$v_d(z) = \frac{1}{R_a(z) + R_b + R_c} \tag{17}$$

where:
$v_d(z)$ – dry deposition velocity on the height z [m s^{-1}],
R_a – aerodynamic resistance on the height z [s m^{-1}],
R_b – laminar layer resistance [s m^{-1}],
R_c – surface resistance [s m^{-1}].

The R_a value depends mainly on the atmospheric turbulence intensity – the higher the turbulence is, the more intensive transport to the surface. The atmospheric resistance to transport of gasses across the constant flux layer is assumed to be similar to that of heat (Erisman, 1992):

$$R_a(z) = \frac{1}{k \cdot u_*}\left[\ln\left(\frac{z}{z_0}\right) - \Psi_h\left(\frac{z}{L}\right) + \Psi_h\left(\frac{z_0}{L}\right)\right] \tag{18}$$

where:
k – von Karman constant [–],
u_* – friction velocity [m s^{-1}],
z_0 – aerodynamical roughness coefficient [m],
L – the Monin-Obukhov length [m],
Ψ_h – integrated stability function for heat [–].

Integrated stability function for heat Ψ_h is calculated as follows (Erisman, 1992):

$$\Psi_h\left(\frac{z}{L}\right) = -5.2\left(\frac{z}{L}\right) \quad \text{for} \quad L > 0\,, \tag{19}$$

and

$$\Psi_h\left(\frac{z}{L}\right) = 2 \cdot \ln\left(\frac{1+x^2}{2}\right) \quad \text{for} \quad L < 0\,, \tag{20}$$

where:

$$x = \left[1 - 16\frac{z}{L}\right]^{\frac{1}{4}}\,.$$

In the sublaminar layer pollutant transport to the surface depends on both turbulence and molecular diffusion of the pollutant and can be approximated as (Erisman, 1992)

$$R_b = \frac{2}{k \cdot u_*}\left(\frac{S_c}{P_r}\right)^{\frac{2}{3}}\,, \tag{21}$$

where:
S_c – Schmidt number [–]; $S_c = \frac{\nu}{D}$, where ν is the kinematic viscosity of air (0.15 cm^2 s^{-1}),
D is the molecular diffusifity of the pollutant [cm^2 s^{-1}],
P_r – Prandtl number [–]; $P_r = 0.72$.

On the surface the absorption of the pollutant is dependent on the component and receptor characteristics. R_c is the function of chemical, biological and physical characteristics of the receptor chemical and physical characteristics of pollutant as well as time of the year and time of day. The R_c value is the most difficult to parameterize. In the RIVM's scheme the measurement of dry deposition taken during EUROTRAC and BIATEX experiments (see Erisman *et al.*, 1992 and Seland *et al.*, 1995) have been used for R_c parameterization. Procedures applied in the dry deposition model are based on Monin-Obukhov theory for surface layer. As in transport model the stability is determinated by Pasquill's stability classes, for the determination of the Monin-Obukhov length (L) the Golder's graphical relationships among the stability parameters have been applied. The friction velocity (u_*) have been calculated due to logarithmic profile (Lyons and Scott, 1990)

$$u_* = k u_a \cdot \left[\ln\left(\frac{z_a}{z_0}\right)\right]^{-1}, \qquad (22)$$

where:
u_a – anemometric wind velocity [m s^{-1}],
z_a – anemometric height [m].

Areodynamical roughness coefficients (z_0) have been prepared for computational grid with resolution of 10 km x 10 km. Annual mean values of z_0 have been calculated from the data taken from ECMWF (European Centre for Medium-Range Weather Forecasts, Reading, UK).

The land-cover data for Poland are essential for the presented work – these data in each computational grid are needed as a input to the dry deposition submodel. The land-cover map for the territory of Poland in the adopted computational grid has been prepared on the base of RIVM's original data (compare Veldkamp and van de Velde, 1995) with geographical resolution of 10' x 10'. A Geographical Information System (Arc/Info) was used to convert original data into a projection and resolution suitable for the adopted computational grid (with resolution 10 km x 10 km). The following land-use categories are included in original data: coniferous and mixed forest, deciduous forest, permanent crops, grassland, urban areas, arable land, inland water, sea and "other". Additional category: "high mountain forest" have been introduced and added to the land-cover prepared for the current work.

Calculations of v_d value have been carried out by the means of dry deposition model described above. As a result, the SO_2 dry deposition velocity map at each node of the computational grid have been obtained, constituting an input for the transport model calculations discussed in Section 1.

3 Simulation of sulfur deposition in Poland

The model has been applied for generating seasonal and annual sulfur deposition resulting from the major power and heating plants of the Polish energy sector. The computational domain is based on EMEP-oriented rectangle 900 km x 750 km containing Poland (compare Fig. 1). The uniform resolution based on the grid element 10 km x 10 km is applied, thus the computational grid has the dimension 90x75. The set of 91 sources taken into account is presented in Table 1. The position of each source in the table is shown in coordinates of this discrete domain. The emissions shown in the last two columns of Table 1 represent quantities averaged over the winter and summer seasons, respectively.

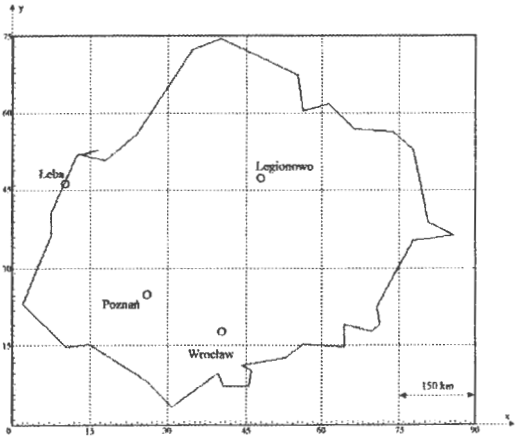

Figure 1: Poland in EMEP coordinates and the main aerological measurement stations

The input to the wind field submodel is based on the spatial and temporal interpolation of the meteorological data from four aerological measurement sites: Poznań, Wrocław, Leba and Legionowo, as shown in Fig. 1. Each station records every 12 hours the following set of data:

- components of the anemometric wind u_A, v_A,
- components of the geostrophic wind (850 hPa) u_G, v_G,
- precipitation intensity
- temperature,
- relative humidity.

Table 1. Characteristics of emission sources (data for the year 1999)

	Power plant	stack	(x,y)-coord. [grid element]	Height [m]	Temp. [°C]	SO_2 emission –winter [Mg h^{-1}]	SO_2 emission –summer [Mg h^{-1}]
1	Bełchatów	1	(48.2, 32.1)	300	153.00	24.1060	12.7226
2	Bełchatów	2	(48.2, 32.1)	300	96.00	13.5983	7.1769
3	Pątnów	1	(35.5, 34.0)	150	145.00	7.3912	3.9009
4	Pątnów	2	(35.5, 34.0)	150	145.00	8.3037	4.3825
5	Adamów	1	(38.8, 33.4)	150	145.00	1.9424	1.0251
6	Konin	1	(35.8, 34.2)	120	150.00	1.7027	.9804
7	Konin	2	(35.8, 34.2)	100	150.00	1.7427	.9195
8	Konin	3	(35.8, 34.2)	100	160.00	1.1490	1.0120
9	Konin	4	(35.8, 34.2)	100	150.00	.0487	.0257
11	Turów	2	(31.6, 5.6)	150	145.00	4.9238	2.5987
12	Turów	3	(31.6, 5.6)	150	145.00	7.3856	3.8979
13	Turów	4	(31.6, 5.6)	150	145.00	5.5392	3.8979
14	Kozienice	1	(55.7, 47.4)	200	120.00	2.2144	1.1687
15	Kozienice	2	(55.7, 47.4)	200	120.00	3.6980	1.9517
16	Kozienice	3	(55.7, 47.4)	300	135.00	2.6504	1.3988
17	Dolna_Odra	1	(9.7, 22.1)	250	104.00	4.7304	2.4966
18	Dolna_Odra	2	(9.7, 22.1)	250	104.00	4.7304	2.4966
19	Pomorzany	1	(8.7, 23.0)	160	150.00	.6395	.3375
20	Połaniec	1	(66.2, 38.3)	250	135.00	6.0830	3.2105
21	Połaniec	2	(66.2, 38.3)	250	135.00	6.0830	3.2105
22	Rybnik	1	(55.7, 19.5)	260	135.00	4.1790	2.2056
23	Rybnik	2	(55.7, 19.5)	300	135.00	4.1790	2.2056
24	Jaworzno_II	1	(59.7, 23.7)	120	150.00	1.5442	.8150
25	Jaworzno_III	1	(58.7, 24.7)	300	130.00	4.1680	2.3996
26	Łaziska	1	(57.7, 21.0)	160	142.00	.4130	.3640
27	Łaziska	2	(57.7, 21.0)	200	140.00	5.0555	2.6682
28	Łagisza	1	(57.5, 24.7)	160	145.00	1.9289	1.0180
29	Łagisza	2	(57.5, 24.7)	200	140.00	2.7863	1.4705
30	Siersza	1	(60.3, 25.3)	150	145.00	1.3190	.6961
31	Siersza	2	(60.3, 25.3)	260	135.00	2.5405	1.3408
32	Ostrołęka_B	1	(42.6, 57.8)	120	105.00	3.2686	1.7251
33	Skawina	1	(63.6, 25.7)	120	148.00	1.4734	.7776
34	Skawina	2	(63.6, 25.7)	120	148.00	1.8010	.9505
35	Stalowa_Wola	1	(68.2, 43.7)	150	145.00	.0350	.0185
36	Stalowa_Wola	2	(68.2, 43.7)	102	145.00	.7006	.3698
37	Stalowa_Wola	3	(68.2, 43.7)	120	145.00	.8571	.4524
38	Blachownia	1	(52.5, 19.1)	102	150.00	.2936	.1549
39	Blachownia	2	(52.5, 19.1)	151	145.00	.6038	.3187
40	Halemba	1	(57.1, 22.2)	110	150.00	1.1275	.5951
41	Miechowice	1	(55.7, 22.6)	68	130.00	.2624	.1385
42	Miechowice	2	(55.7, 22.6)	68	130.00	.2624	.1385
43	Opole	1	(48.1, 20.4)	250	130.00	.7508	.5284
44	Szczecin	1	(8.8, 23.6)	100	104.00	.4226	.0921
45	Szczecin	2	(8.8, 23.6)	100	104.00	.3323	.0000
46	Zielona_Góra	1	(25.7, 16.8)	60	160.00	.2075	.0736

Table 2 (continued). Characteristics of emission sources (data for the year 1999)

	Power plant	stack	(x,y)-coord. [grid element]	Height [m]	Temp. [°C]	SO_2 emission -winter [Mg h^{-1}]	SO_2 emission -summer [Mg h^{-1}]
47	Zielona_Góra	2	25.7, 16.8	80	160.00	.3535	.0000
48	Gorzów	1	18.1, 21.7	125	115.00	.4272	.0449
49	Gorzów	2	18.1, 21.7	150	115.00	.6536	.1744
50	Poznań_Garbary	1	28.9, 27.9	100	123.00	.4752	.0880
51	Poznań_Karolin	1	28.4, 27.7	200	140.00	1.2744	.3671
52	Bydgoszcz_I	1	27.0, 38.5	100	120.00	.4118	.0681
53	Bydgoszcz_II	1	27.4, 38.8	73	115.00	2.0840	.0179
54	Bydgoszcz_III	1	27.0, 38.8	100	150.00	.8088	.4055
55	Gdynia_II	1	20.4, 49.2	83	155.00	.2634	.0075
56	Gdynia_III	1	17.0, 52.0	150	115.00	1.7135	.4110
57	Gdańsk_II	1	18.6, 51.5	120	120.00	.9550	.3127
58	Gdańsk_II	2	18.6, 51.5	120	180.00	1.1368	.0000
59	Gdańsk_II	3	18.6, 51.6	200	135.00	.7275	.0718
60	Elbląg	1	23.6, 53.9	100	120.00	.5047	.0726
61	Czechnica	1	40.9, 18.3	135	120.00	.5418	.0455
62	Czechnica	2	40.9, 18.3	110	120.00	.5419	.0455
63	Wrocław	1	40.5, 18.4	120	125.00	1.1317	.1931
64	Wrocław	2	40.5, 18.4	180	110.00	2.5671	.3863
65	Kalisz_Piwonice	1	39.9, 29.0	80	150.00	.3497	.0548
66	Łódź_I	1	45.5, 36.8	45	145.00	.3392	.0020
67	Łódź_II	1	45.9, 36.9	120	115.00	1.0648	.1845
68	Łódź_II	2	45.9, 36.9	120	115.00	1.6009	.1976
69	Łódź_III	1	45.6, 36.6	120	115.00	1.7998	.3825
70	Łódź_IV	1	45.8, 36.2	200	125.00	2.7943	.3507
71	Łódź_IV	2	45.8, 36.2	250	120.00	.8567	.2155
72	Ostrołęka_A	1	42.6, 57.9	100	125.00	1.4992	.2502
73	Bedzin	1	57.4, 24.4	150	135.00	1.1395	.2751
74	Chorzów	1	57.3, 23.2	170	115.00	1.0952	.1940
75	Chorzów	2	57.3, 23.2	101	115.00	.5071	.0000
76	Szombierki	1	55.9, 23.2	120	135.00	.0791	.0058
77	Szombierki	2	55.9, 23.2	115	150.00	.0235	.0000
78	Szombierki	3	55.9, 23.2	115	150.00	.0295	.0000
79	Zabrze	1	55.9, 22.3	95	130.00	1.2231	.3868
80	Zabrze	2	55.9, 22.3	200	130.00	1.0384	.0000
81	Powiśle	1	48.2, 48.8	31	165.00	.3739	.0027
82	Pruszków_I	1	48.1, 47.3	27	140.00	.3457	.0058
83	Żeran	1	47.6, 49.2	100	120.00	1.0219	.2438
84	Żeran	2	47.6, 49.2	100	120.00	1.0219	.2438
85	Żeran	3	47.6, 49.2	200	120.00	1.1565	.0000
86	Siekierki	1	48.8, 49.0	120	115.00	1.6955	.2773
87	Siekierki	2	48.8, 49.0	200	120.00	5.1169	.8153
88	Białystok	1	48.6, 67.1	120	120.00	1.2201	.3123
89	Bielsko-Biała	1	62.1, 21.3	160	120.00	1.2898	.2524
90	Kraków_Łęg	1	63.8, 27.0	225	120.00	2.5703	.5553
91	Kraków_Łęg	2	63.8, 27.0	260	120.00	1.9857	.3704

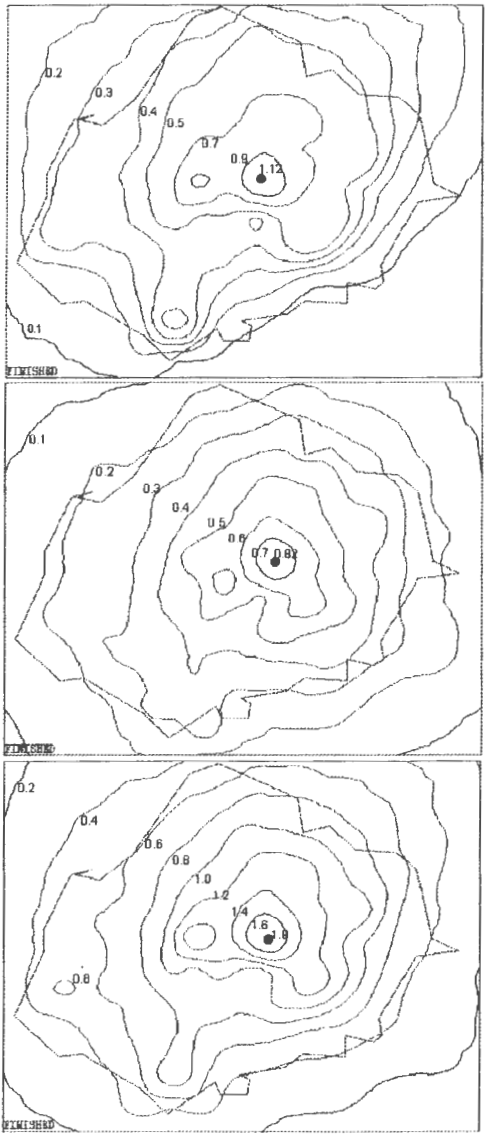

Figure 2: Total sulfur deposition in 1999 [g(S) m^{-2}] for constant $v_d = 0.008$ m s^{-1}
a) winter season, b) summer season, c) annual

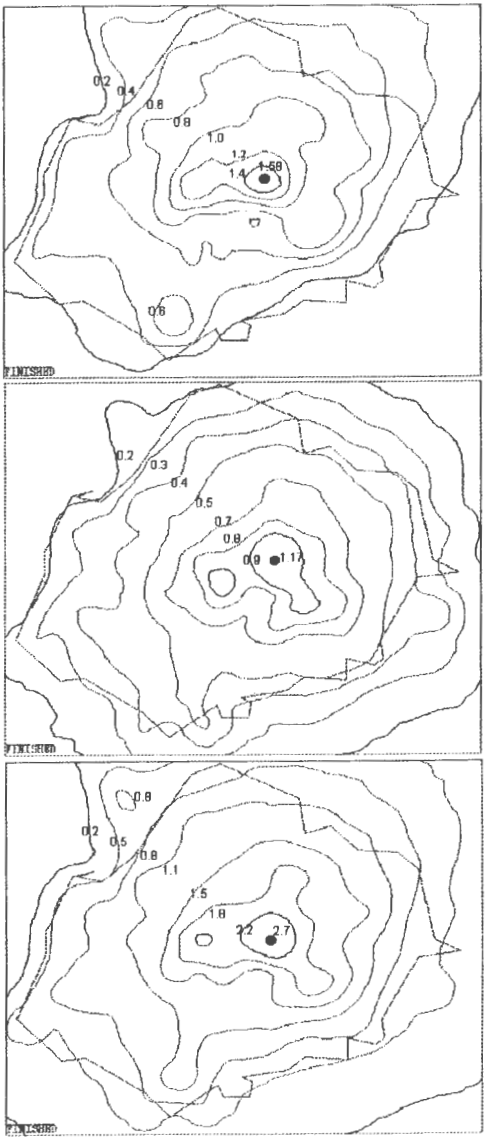

Figure 3: Total sulfur deposition in 1999 [g(S) m^{-2}] for RIVM dry deposition model a) winter season, b) summer season, c) annual

The above data have to be spatially and temporarily interpolated over the computational domain, according to the procedure discussed in Section 1. The wind field, in this case, is preprocessed by the spatial interpolation of the measured input data of four stations shown in Fig. 1, and temporal interpolation of the consecutive sets of data.

The assumed linearity of the dispersion process (linear dependence of the concentration with respect to the emission intensity of the source) allows us to simulate separately the environmental impact of all the sources under consideration. Then, the total deposition map can be then calculated as a superposition of those individual contributions.

Results of computation shown in Figures 2 – 3 present sulfur deposition maps, obtained for two methods of dry deposition parameterization. The first one is related to constant value of dry deposition velocity, v_d=0.008 [m s^{-1}]. The other map presents results obtained for variable (in space and time) dry deposition velocity, computed by the built-in RIVM procedure, discussed in Section 3. As one can see, the maximum deposition values near the dominating sources are substantially higher when variable deposition velocity is applied.

4 Conclusions

The parameterization of the dry deposition velocity (v_d) is very important in air dispersion models as both concentration and deposition values strongly depend on that value. For this purpose, to improve predictions of the transport model, the specialized dry deposition submodel has been built in and analyzed. The dry deposition submodel for sulfur species has been developed and tested, based on the original multi-species RIVM's (the National Institute of Public Health and Environmental Protection, Bilthoven, the Netherlands) dry deposition model (Seland *et al.*, 1995).

It is known, and confirmed by the presented maps, that the sulfur deposition in Poland is rather high. It should be mentioned that the total (from all sources) sulfur emission in Poland in the years 1985 – 1997 has been reduced almost twice (from 4300 Gg SO_2 in 1985 to 2181 Gg SO_2 in 1997). Nevertheless, the emission is still substantial on the European scale, and the resulting deposition is still higher than the critical loads for sulfur. The total (dry + wet) sulfur deposition for the whole country, related to emission sources shown in Table 1, counts: 390 Gg (S) when using constant value of dry deposition velocity (Figure 2) and 535 Gg (S), when using RIVM's dry deposition model for calculating variable in time and space dry deposition velocities (Figure 3).

Thus, the total annual sulfur deposition for Poland calculated by using dry deposition model is about 27 % higher than the deposition calculated by using constant value of v_d. Taking into account the seasonal distributions of total deposition in Poland it can be noted that in both calculations the values for the winter season are higher that those for the summer season. This is strictly connected with the annual distribution of emission – in winter (so-called "heating season") emissions from the majority of power stations are almost twice higher than those in the summer season.

The built-in dry deposition model (Figure 3) generates higher values of deposition,

especially in the neighborhoods of the major emission sources. One can distinguish the following areas of extremal total annual values: the surroundings of Bełchatów electric power station – central part of Poland, with the maximum deposition of 1.9 – 2.7 g(S) m^{-2} yr^{-1} and the surroundings Turów electric power station (the border of Poland, the Czech Republic and Germany, region of the Karkonosze mountains) with the maximum deposition of 0.9 – 1.4 g(S) m^{-2} yr^{-1}. The respectively higher deposition values are related to variable v_d case (compare Figure 2 and Figure 3).

There are also differences in the resulting spatial distributions of sulfur deposition in both algorithms. RIVM's model, for example, shows a remarkable influence of Gdańsk power stations on the East Baltic region, while this effect is not indicated by the other approach. On the other hand, the lower deposition for the constant v_d case, causes respectively higher concentrations of SO_2 in regions of major sources location and higher impact on distant receptors.

It must be also noted, that the implementation of RIVM deposition algorithm causes a substantial increase of the computing time of the entire transport model (about four times comparing to that of the constant v_d case), since additional computations have to be performed in all grid elements in the consecutive time steps. The computing time is not, however, a critical factor in the annual deposition analysis. On the other hand, the substantial differences between both results suggest, that utilizing the variable dry deposition approach gives more realistic and accurate results, which is important for resulting accuracy of dispersion and deposition models.

Acknowledgements. Authors are grateful to Dr J.W. Erisman and Dr A. van Pul from RIVM (National Institute of Public Health and Environmental Protection, Bilthoven, the Netherlands) for giving access to the original version of multi-species dry deposition model (DEPAC).

This research was partially supported by the ESPRIT Project 20288 Cooperation Research in Information Technology (CRIT2): "Evolutionary Real-time Optimization System for Ecological Power Control".

REFERENCES

Erisman J.W. (1992) Atmospheric deposition of acidifying compounds in the Netherlands. PhD-thesis. University of Utrecht, the Netherlands.

Erisman J.W., van Pul W.A.J. and Wyers G.P. (1994) Parameterization of surface resistance for the quantification of atmospheric deposition of acidifying pollutants and ozone. *Atmospheric Environment* **28**, 2595-2607.

Golder D. (1972) Relations among stability parameters in surface layer. *Boundary Layer Meteorology* **3**, 47-58.

Lyons T.J. and Scott W.D. (1990) *Principles of Air Pollution Meteorology.* Belhaven Press, London.

Sandnes H. (1993) Calculated budgets for airborne acidifying components in Europe. Report EMEP/MSC-W, 1/93. The Norwegian Meteorological Institute, Oslo.

Seland Ø., Van Pul A., Soteberg A. and Touvinen J-P. (1995) Implementation of a Resistance Dry Deposition Module and Variable Local Correction Factor in the Lagrangian EMEP Model. Report EMEP/MSC-W, 3/95. The Norwegian Meteorological Institute, Oslo.

Van Pul A. (1994) Dry deposition model (FORTRAN code, DEPAC). Report LLO/RIVM, Bilthoven, the Netherlands.

Veldkamp H. and van de Velde R. (1995) Mapping Land Use and Land Cover for Environmental Monitoring on a European Scale. In *Calculation and mapping of critical tresholds in Europe* (eds.: Posch M., de Smet P.A.M., Hettelingh J.-P. and Downing R.J.), CCE Status Report 1995, RIVM rep. 259101004, Bilthoven, Netherlands, 51-60.

Voldner E.C., Barrie L.A. and Sirois A. (1986) A literature review of dry deposition of oxides of sulfur and nitrogen with emphasis on long-range transport modeling in North America. *Atmospheric Environment* **20**, 2101-2133.